Atmospheric and Oceanic Science Letters

ISSN: 1674-2834 (Print) 2376-6123 (Online) Journal homepage: https://www.tandfonline.com/loi/taos20

Interannual variability in the onset of the South China Sea summer monsoon from 1997 to 2014

Bian HE, Ying ZHANG, Ting LI & Wen-Ting HU

To cite this article: Bian HE, Ying ZHANG, Ting LI & Wen-Ting HU (2017) Interannual variability in the onset of the South China Sea summer monsoon from 1997 to 2014, Atmospheric and Oceanic Science Letters, 10:1, 73-81, DOI: 10.1080/16742834.2017.1237853

To link to this article: https://doi.org/10.1080/16742834.2017.1237853

ATMOSPHERIC AND OCEANIC SCIENCE LETTERS, 2017
VOL. 10, NO. 1, 73–81
http://dx.doi.org/10.1080/16742834.2017.1237853

Taylor & Francis
Taylor & Francis Group

Interannual variability in the onset of the South China Sea summer monsoon from 1997 to 2014

HE Bian[a], ZHANG Ying[b], LI Ting[a] and HU Wen-Ting[a]

[a]State Key Laboratory of Numerical Modeling for Atmospheric Sciences and Geophysical Fluid Dynamics, Institute of Atmospheric Physics, Chinese Academy of Sciences, Beijing, China; [b]Weather Station, Suqian Meteorological Administration, Suqian, China

ABSTRACT

Using observed and reanalysis datasets, the South China Sea summer monsoon (SCSSM) onset process is analyzed in each year from 1997 to 2014. Regional mean (5–20°N, 110–120°E) 850 hPa zonal wind, precipitation, and SST are used as indices to describe SCSSM onset. Three distinct onset types are identified: among the 18 years studied, nine are normal onset years, which are characterized by a well-established westerly wind and associated precipitation over the South China Sea (SCS); eight are intermittent onset years, in which monsoon precipitation does not occur continuously following the establishment of the westerly wind over the SCS; and one year, 2014, is a delayed onset year, in which the western Pacific subtropical high dominates over the SCS after the seasonal transition and prevents the monsoon onset. A comparison of the first two types suggests that a positive SST gradient in the northern Indian Ocean and local SST warming in the SCS are two key factors in the normal SCSSM onset type. With regard to the influence of the El Niño–Southern Oscillation background, there are four late onset years (1997, 1998, 2007, and 2010) that coincide with El Niño events, but only two early-onset years (1999 and 2012) out of the six years featuring La Niña events. Further analysis suggests that the zonal thermal contrast across the Indian and western Pacific oceans modulates monsoon onset in La Niña years.

摘要

本文基于南海地区850 hPa风场，降水以及海温定义了南海夏季风爆发指数，将南海季风爆发过程分为季节转换和季风爆发两个过程来进行研究。对18年的观测分析发现，南海季风爆发可归纳为三种情况：第一种是季风正常爆发，随着季节转换结束后，西南季风和降水在南海地区有明显增强；第二种是间接性爆发，在季节转换结束后，西南季风和降水的建立不是特别明显；第三种是推迟爆发，在季节转换结束后，南海地区没有建立西南季风也没有降水产生。进一步研究发现，西太副高异常西伸是导致南海季风延迟爆发的重要因素之一。此外，大尺度环流背景ENSO的影响也对南海季风爆发时间的早晚有重要影响，但并不是唯一决定性因素，印度洋和亚洲大地形的局地热力差异变化是影响季风爆发的另一重要因素。

ARTICLE HISTORY
Received 26 April 2016
Revised 3 August 2016
Accepted 17 August 2016

KEYWORDS
South China Sea; summer monsoon onset; air–sea interaction

1. Introduction

The South China Sea summer monsoon (SCSSM) is one of the most important components of the Asian summer monsoon (ASM) system. It links the Bay of Bengal (BOB) summer monsoon and the East Asian summer monsoon through its geographical location, and it exhibits features characteristic of both the tropical and subtropical monsoons (Wang et al. 2004). In general, ASM onset occurs first over the southeastern BOB, from late April to early May, followed by the South China Sea (SCS) in mid-May, and finally over India from late May to early June (Wu and Zhang 1998; Wang and Lin 2002; Liu et al. 2015). However, obtaining a generalized definition of SCSSM onset remains challenging, since the SCSSM exhibits considerable interannual variability (Wu and Wang 2001). Several factors contribute to this complexity, including El Niño–Southern Oscillation (ENSO) effects (Lau and Nath 2000; Hu, Wu, and Liu 2014), regional air–sea interactions (Wang, Wu, and Li 2003; He and Wu 2013), and active intraseasonal oscillations (ISOs) (Mao and Chan 2005; Wen et al. 2010).

Indices describing SCSSM onset introduced in previous studies can be broadly classified into three types,

CONTACT HE Bian heb@lasg.iap.ac.cn
The supplemental data for this paper is available online at http://dx.doi.org/10.1080/16742834.2017.1237853.

each involving a different dynamical atmospheric variable. The first of these is 850 hPa wind velocity, which measures the strength of southwesterlies over the SCS (Hsu, Terng, and Chen 1999; Wang et al. 2004); the second is precipitation, or its proxies, outgoing longwave radiation or cloud top brightness temperature, which indicate the formation of deep convective systems over the SCS (Lin and Lin 1997; Xie et al. 1998); the third type looks for the systematic reversal of the atmospheric meridional thermal contrast, measured as the area-averaged meridional-mean upper-tropospheric (200–500 hPa) temperature gradient in the vicinity of the ridge of the subtropical anticyclone (Mao, Chan, and Wu 2004). Wang et al. (2004) summarized these index types and suggested a simple and effective index: 850 hPa zonal wind (U_{850}) averaged over the central SCS (5–15°N, 110–120°E). This index shows good correlation between the establishment of the tropical southwesterly monsoon and the outbreak of the rainy season over the entire SCS. However, there are some years in which onset is harder to define, when the cessation of the easterly regime is not immediately followed by the establishment of a coherent westerly regime (Wang et al. 2004). This may be due to a delayed atmospheric circulation response to SST anomalies, linked to ocean–atmosphere interactions including wind–evaporation and cloud–radiation effects (Wu 2010). It is therefore necessary and instructive to seek to understand SCSSM onset by studying the simultaneous evolution of the monsoon circulation, SST, and precipitation on the subseasonal timescale over the SCS in individual years.

In this study, we use observed daily precipitation and SST together with reanalysis data from 1997 to 2014 to study the interannual variability of the SCSSM onset process. The thermodynamical relationships between SCSSM circulation and precipitation in each year are analyzed, and four indices are calculated to quantitatively describe the SCSSM onset process. Onset is classified into three types and its main features are analyzed. The remainder of the paper is organized as follows: Section 2 introduces the datasets used; Section 3 presents the analysis of SCSSM onset and its interannual variability; and Section 4 summarizes the results.

2. Datasets

The precipitation data-set used in the study is the GPCP 1-Degree Daily Combination (version 1.2) data-set (Huffman et al. 2001). The GPCP data-set has a spatial resolution of 1° × 1° and is available from October 1996 to the present. This data-set is provided by the GPCP Global Merge Development Centre, based in the NASA/GSFC Mesoscale Atmospheric Processes Laboratory (http://precip.gsfc.nasa.gov/).

JRA-55 (Kobayashi et al. 2015) is used to obtain multi-level geopotential height, vertical velocity, and winds on a 1.25° × 1.25° grid. This data-set covers the period from 1958 to the present day. The data-set is available at http://jra.kishou.go.jp/JRA-55/index_en.html.

The NOAA high-resolution blended analysis of daily SST (Reynolds et al. 2007) is also used. This data-set covers the period from September 1981 to the present day, and is available at http://www.esrl.noaa.gov/psd/data/gridded/data.noaa.oisst.v2.highres.html.

3. Results

Figure 1 shows the evolution of U_{850} and precipitation, averaged over the SCS (110–120°E), for each year from 1997 to 2014. A five-day running mean has been applied to the daily data to remove high-frequency variability. In general, a strong easterly wind prevails over 5°–20°N from March to May in almost all years, which indicates that the winter circulation regime is still well-maintained over the SCS during spring. Meanwhile, strong precipitation (greater than 6 mm d^{-1}, overlaid with hatched contours in Figure 1) is located mainly over the ITCZ. In the subtropical region (20–30°N), a series of episodes of westerly wind and associated precipitation occur throughout boreal spring, which can be described as 'early spring rainfall over South China'. SCSSM onset usually occurs after April, and is characterized by the sudden reversal of U_{850} direction in the 5–20°N band, often accompanied by a propagation of continuous precipitation from the southern SCS to the northern SCS. Note that outbreaks of strong precipitation are consistent with the appearance of U_{850} over the SCS and the South China mainland in all years, which indicates that JRA-55 captures the SCSSM onset process well and lays a solid physical foundation for the analysis that follows.

The end point of the easterly wind regime can be regarded as the date of the seasonal transition over the SCS. In contrast to the predictable evolution of the easterly wind at 5–20°N, the arrival of westerly winds varies considerably from year to year. This onset can be roughly divided into two types. One type involves a sudden onset after the seasonal transition, and is characterized by a westerly wind that is rapidly established and subsequently maintained, along with strong precipitation, after the end of the period of continuous easterly wind, such as in 1997 (Figure 1(a)), 1998 (Figure 1(b)), 2002 (Figure 1(f)), 2003 (Figure 1(g)), and 2004 (Figure 1(h)). The other type involves a less sharply defined onset. For example, the onset is weak or delayed by several days after the continuous easterly wind period ends in 2005 (Figure 1(i)), 2007 (Figure 1(k)), 2011 (Figure 1(o)), 2012 (Figure 1(p)), 2013 (Figure 1(q)), and 2014 (Figure 1(r)). Onset may alternatively exhibit one or more reversals in wind direction after the seasonal transition.

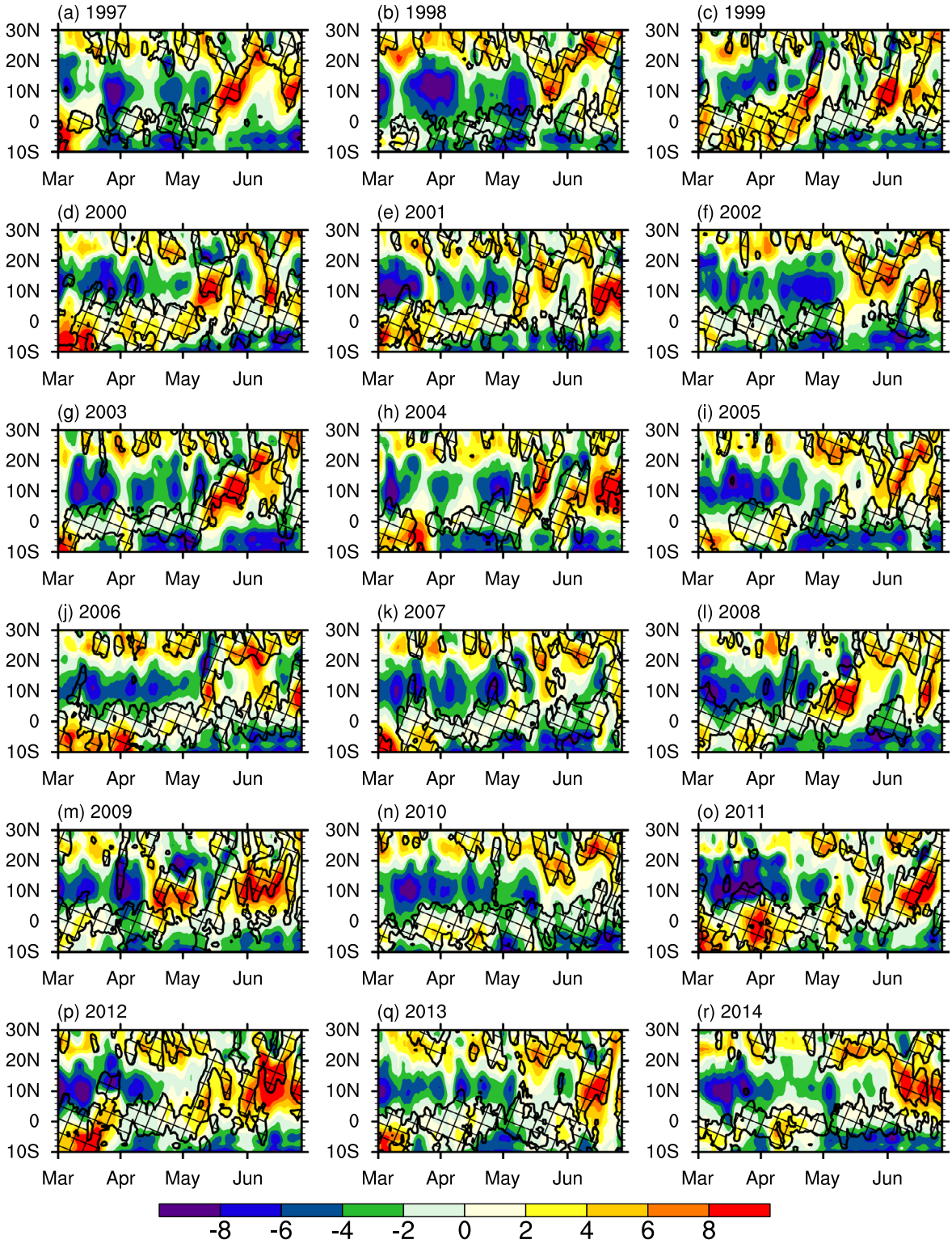

Figure 1. Latitude–time cross sections of the five-day running mean of 850 hPa wind (shading; units: m s^{-1}) and precipitation (hatched; contours of 6 mm dy^{-1}), averaged over 110–120°E, for (a–r) 1997 to 2014.

For example, in 1999 (Figure 1(c)), the continuous easterly wind ceases in late April when it is interrupted by the active ISO propagating from the southern tropics into the SCS in early May. After the ISO ends, easterly winds again prevail over the SCS in mid-May, before the second onset of the SCSSM occurs at the beginning of June. Another different case is 2009 (Figure 1(m)), when a strong westerly wind is established immediately in mid-April, but is then

interrupted by easterlies propagating from the northern SCS for a number of days in early May, before a second westerly outbreak occurs near the end of May.

To gain a clearer and more quantitative understanding of SCSSM onset dynamics, it is necessary to define objective indices that capture the major features of SCSSM onset. Starting with the one-dimensional index of U_{850} averaged over (5–15°N, 110–120°E), created by Wang et al. (2004), we extend the northern boundary to 20°N to include the northern part of the SCS, since the onset process occurs in this region in some years. In Figure 2, we plot five-day running mean time series of U_{850}, SST, and precipitation, averaged over the region defined above (marked as a black box in Figure 3(a)). Composite spatial distributions for the onset state for each are shown in Figure S1. These three variables together depict both thermal and dynamical aspects of the SCSSM onset process.

Several common features can be seen in all 18 years: easterly wind ($U_{850} < 0$) is maintained for around 45–60 days from the beginning of March; meanwhile, SST increases to a maximum, and then drops suddenly when the westerly wind rapidly intensifies, accompanied by sharply increased rainfall. In some years the SST reaches its maximum before the peak in precipitation occurs, which may be due to the time lag between SST anomalies and the atmospheric convective response (Wu 2010). It is interesting to note that in most years the SST reaches its maximum prior to the beginning of a period of near-continuous rainfall following SCSSM onset. Therefore, the date of the SST maximum can be regarded as a good index by which to identify the SCSSM onset process from a thermodynamical perspective. Difficulty remains in identifying the systematic establishment of westerly wind over the SCS. For example, westerly winds are clearly established after the reversal

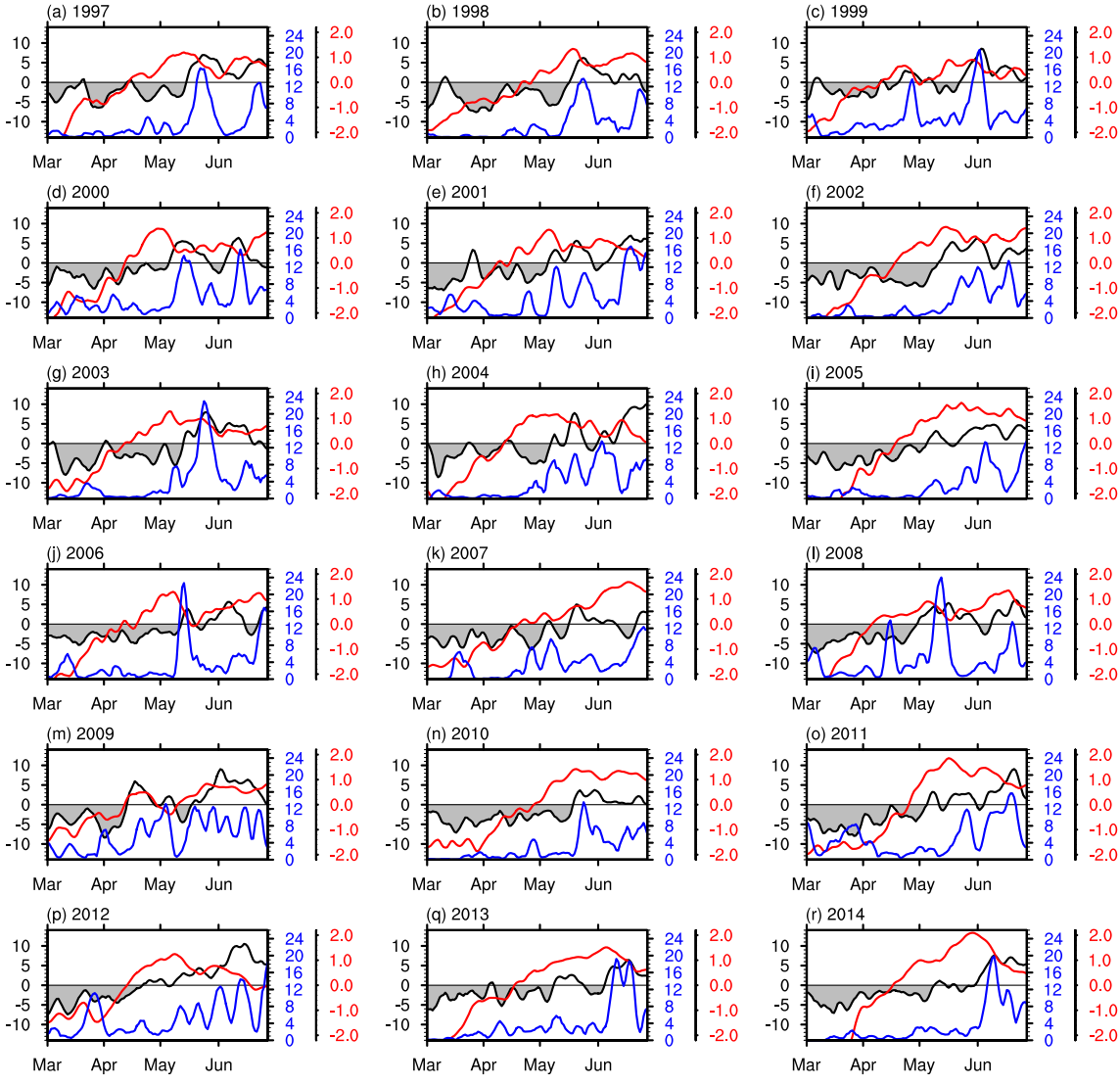

Figure 2. Time series of 850 hPa zonal wind (black; units: m s^{-1}), precipitation (blue; mm d^{-1}), and SST (red; units: K), averaged over (5–20°N, 110–120°E), for (a–r) 1997 to 2014. Gray shaded areas denote periods of easterly wind.

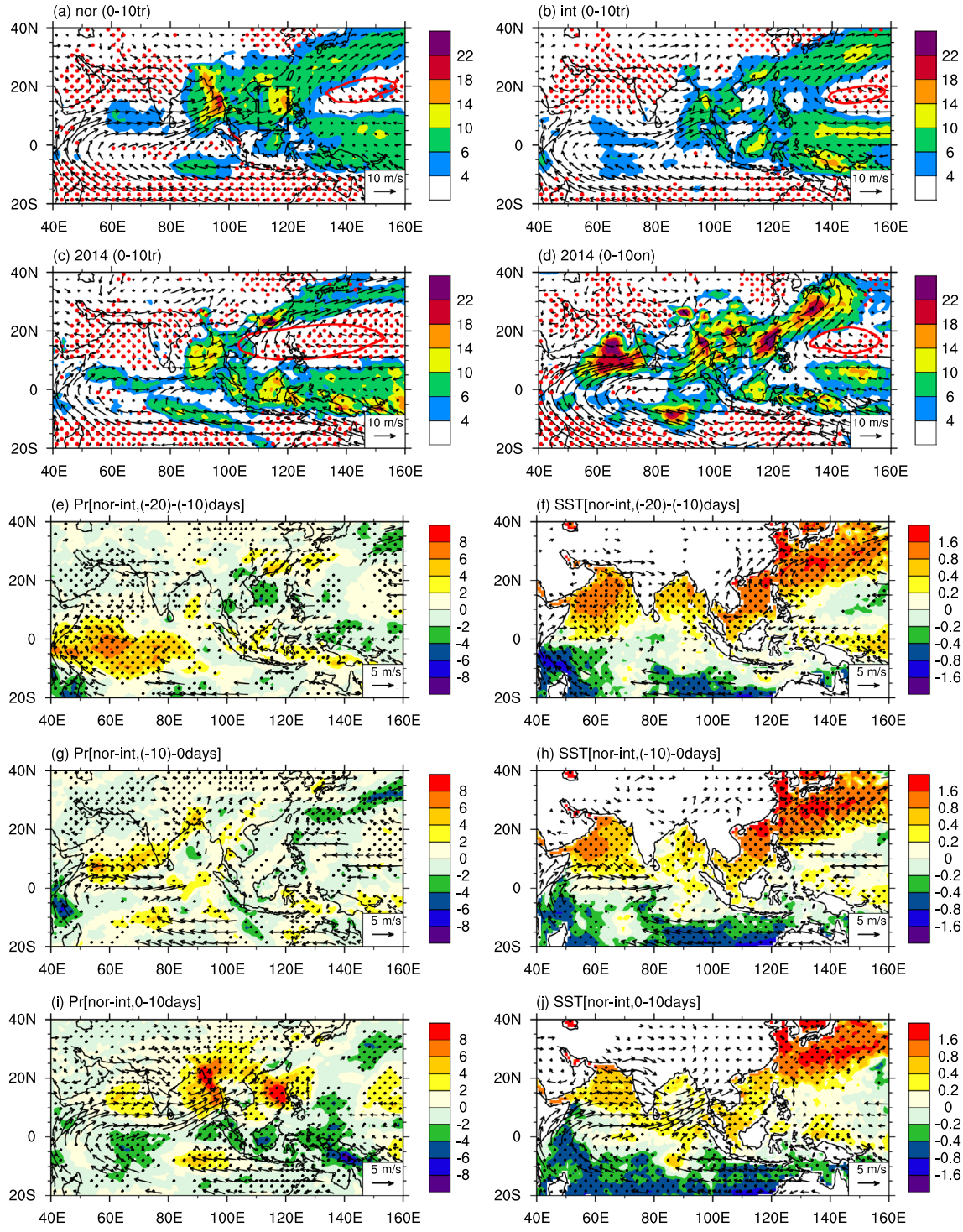

Figure 3. (a) Precipitation (shading; units: mm d^{-1}) and 850 hPa wind (vectors; units: m s^{-1}) averaged over 10 days starting at TRD for the normal onset cases. Red dots mark descending motion (vertical velocity > 0.2 hPa s^{-1}) at 500 hPa, and the red contour denotes the 5,875 gpm geopotential height. (b) As in (a) but for the intermittent onset cases. (c) As in (a) but for the delayed onset case. (d) As in (c) but averaged over 10 days starting at OND. (e) Difference in precipitation (shading; units: mm d^{-1}) and 850 hPa wind (vectors; units: m s^{-1}), averaged between 20 and 10 days before TRD, between the normal onset and intermittent onset types. Black dots mark precipitation values that have passed the 0.05 significance test. (f) As in (e) but for SST (shading; units: K). (g, h) As in (e, f) but for averages over the 10 days preceding TRD. (i, j) As in (e, f) but for averages over the 10 days following TRD.

of U_{850} in mid-May in 1997 (Figure 2(a)) and 1998 (Figure 2(b)), but westerly winds are weak and ambiguous after the reversal of U_{850} in early May in 2014 (Figure 2(r)). In the latter case, strong and sustained westerly winds occur at the beginning of June, after the SST maximum, and are accompanied by heavy rainfall. Therefore, it is helpful to

separate the evolution of U_{850} into a seasonal transition phase and an SCSSM onset phase, to attempt to gain a clearer physical understanding of the process. SST and precipitation indices are also defined to aid identification of the SCSSM onset date. In this way, the SCSSM onset process can be classified according to its thermodynamical features. We make four definitions, as follows:

(1) Seasonal transition date (TRD): The date when systematic easterly winds over the SCS cease, and the atmospheric circulation moves from winter to summer regime. TRD is defined as the first day i on which ($U^i_{850} > 0, U^{i-1}_{850} < 0$), the wind is easterly on at least 25 of the previous 30 days before i, and the wind is easterly on fewer than 5 of the next 10 days.

(2) Westerly wind onset date (OND): The date when systematic westerly winds are clearly established over the SCS. OND is defined as the first day i on which $U^i_{850} > 0$, the wind is westerly on at least 15 of the next 20 days after i, and the mean U_{850} is greater than 1 m s^{-1} throughout the next 20 days.

(3) SST maximum date (SSTD): The date when SST reaches its March–June maximum.

(4) Precipitation onset date (PRD): The date in the March–June period when continuous monsoon precipitation commences. PRD is defined as the first day i after TRD when the mean precipitation over the next 5 days is greater than 2 mm d^{-1} and the maximum precipitation over the next 5 days is greater than 8 mm d^{-1}.

Based on the above definitions, the indices TRD, OND, SSTD, and PRD are calculated for each year, and the results are shown in Table 1. El Niño (La Niña) years are colored red (blue), according to CPC definitions (detailed definitions can be found at http://www.cpc.ncep.noaa.gov/products/analysis_monitoring/ensostuff/ensoyears.shtml). It is clear that OND is generally consistent with TRD, except in 2014 when OND is 20 days later than TRD. Of the 18 years studied, there are three years (1999, 2009, and 2012) when SCSSM onset occurs relatively early, in late April, and four years (1997, 1998, 2007, and 2010) when SCSSM onset occurs relatively late, in late May. In other years, SCSSM onset occurs in mid-May, which is consistent with the statistics of Kajikawa and Wang (2011), who found that the onset date of SCSSM was usually in mid-May over the period 1994–2008. PRD is close to OND in most of the years, but SSTD is late in a number of years, which is related to the ambiguous onset process mentioned previously. Therefore, by considering TRD, OND, SSTD, and PRD together, we divide the SCSSM onset into three types:

Table 1. The TRD (seasonal transition date), OND (westerly wind onset date), SSTD (SST maximum date), and PRD (precipitation onset date) indices, as defined in Section 3 of the main text. El Niño (La Niña) years are marked with a '+'('–') on the superscript, according to CPC definitions. The intermittent onset years are marked with a '*' on the superscript, and the delayed onset year is marked with a '**' on the superscript.

	TRD	OND	SSTD	PRD
1997	17 May	17 May	15 May	17 May
1998^{+}	19 May	19 May	20 May	19 May
1999^{-*}	21 April	21 April	31 May	21 April
2000^{-}	7 May	7 May	1 May	7 May
2001^{-}	7 May	7 May	7 May	7 May
2002	13 May	13 May	16 May	19 May
2003^{+}	15 May	15 May	7 May	16 May
2004	8 May	8 May	11 May	8 May
2005^{+*}	7 May	7 May	25 May	31 May
2006	14 May	14 May	9 May	14 May
2007^{+*}	18 May	18 May	20 June	18 June
2008^{-*}	1 May	1 May	20 June	4 May
2009^{*}	14 April	14 April	28 May	15 April
2010^{+}	21 May	21 May	22 May	21 May
2011^{-*}	7 May	7 May	18 May	20 May
2012^{-*}	23 April	24 April	10 May	8 May
2013^{*}	10 May	10 May	7 June	5 June
2014^{**}	11 May	2 June	31 May	2 June

(1) Normal onset: In these years, TRD, OND and PRD are generally close to one another, while SSTD is no more than three days later than OND. The monsoon westerly is firmly established and deep convection is immediately triggered over the SCS. These years are shown in Table 1 without marking.

(2) Intermittent onset: In these years, TRD and OND are similar, but SSTD or PRD are significantly later than TRD and OND (by their differences having passed a 0.01 significance test; see Figure S2a and b). The delay is caused by a synoptic system, such as an active ISO or northern cold air, entering the SCS. These years are marked with a '*' on the superscript in Table 1.

(3) Delayed onset: In these years, OND is significantly later than TRD, suggesting that the westerly is not firmly established after the seasonal transition. In our study, we find that 2014 satisfies this special case: no strong ENSO background is present, but OND is 20 days later than TRD. This year is marked with a '**' on the superscript in Table 1.

Figure 3(a)–(c) shows the mean state over the 10-day period starting at TRD, for each of the three types. Because the transition date is the same as the onset date in the first two types, the mean state at the seasonal transition, shown in Figure 3(a) and (b), also represents the monsoon onset state for normal and intermittent onset years, respectively. It is clear that the Somali jet is well established in both

normal and intermittent onset years, and westerly wind prevails over South Asia and turns into the North Pacific through the edge of the western Pacific subtropical high (WPSH). Precipitation, on the other hand, shows quite different patterns between the two types: there are clearly two separate precipitation centers, located over the BOB and the SCS, in the normal onset years, but precipitation is weak and vanishes over the SCS in the intermittent onset years. For the special delayed onset case of 2014, we compare the 10-day-mean circulation patterns after TRD (Figure 3(c)) and after OND (Figure 3(d)). It is clear that the southwesterly wind shifts north to the South China mainland, leading to strong local precipitation, while the SCS is dominated by the extension of the WPSH, as the huge anticyclone leads to large-scale descending motion (marked in the figure by red dots) over the entire SCS and delays the local monsoon onset. The strong WPSH remains over the SCS after TRD in 2014, before retreating to the far western Pacific (Figure 3(d)) almost 20 days after TRD, which finally allows SCSSM onset in early June.

The normal onset and intermittent onset types are by far the most common of the three. We further examine the differences between these two types to try to explain their behavior from a thermodynamical perspective. Figure 3(e) and (f) shows the differences in precipitation, 850 hPa winds, and SST, averaged between 20 and 10 days before TRD, between the normal and intermittent onset types. A clear pattern of warmer SST in the Arabian Sea, BOB, SCS, and northwestern Pacific, and cooler SST in the South Indian Ocean and elsewhere in the Southern Hemisphere, is seen for the normal onset type. The meridional thermal contrast is strong over the western Indian Ocean and leads to an enhanced Somali jet and increased precipitation (Figure 3(e)). In the 10 days preceding TRD, the thermal contrast over the tropical Indian Ocean from 80 to100°E (Figure 3(h)) is stronger than in the previous 10 days (Figure 3(f)), which favors the generation of southwesterly winds locally. In addition, the precipitation belt shifts northward, associated with the enhanced westerly wind in the western Indian Ocean (Figure 3(g)). Finally, during the 10 days following the monsoon onset, cooler SST covers the entire southern Indian Ocean (Figure 3(j)), which enhances the meridional thermal contrast, significantly intensifying the southwesterly flow and contributing to strong precipitation over the BOB and SCS (Figure 3(i)). It is also worth noting that the SST difference is more than 0.8 °C over the SCS during the 20 days preceding the monsoon onset, which favors the triggering of precipitation

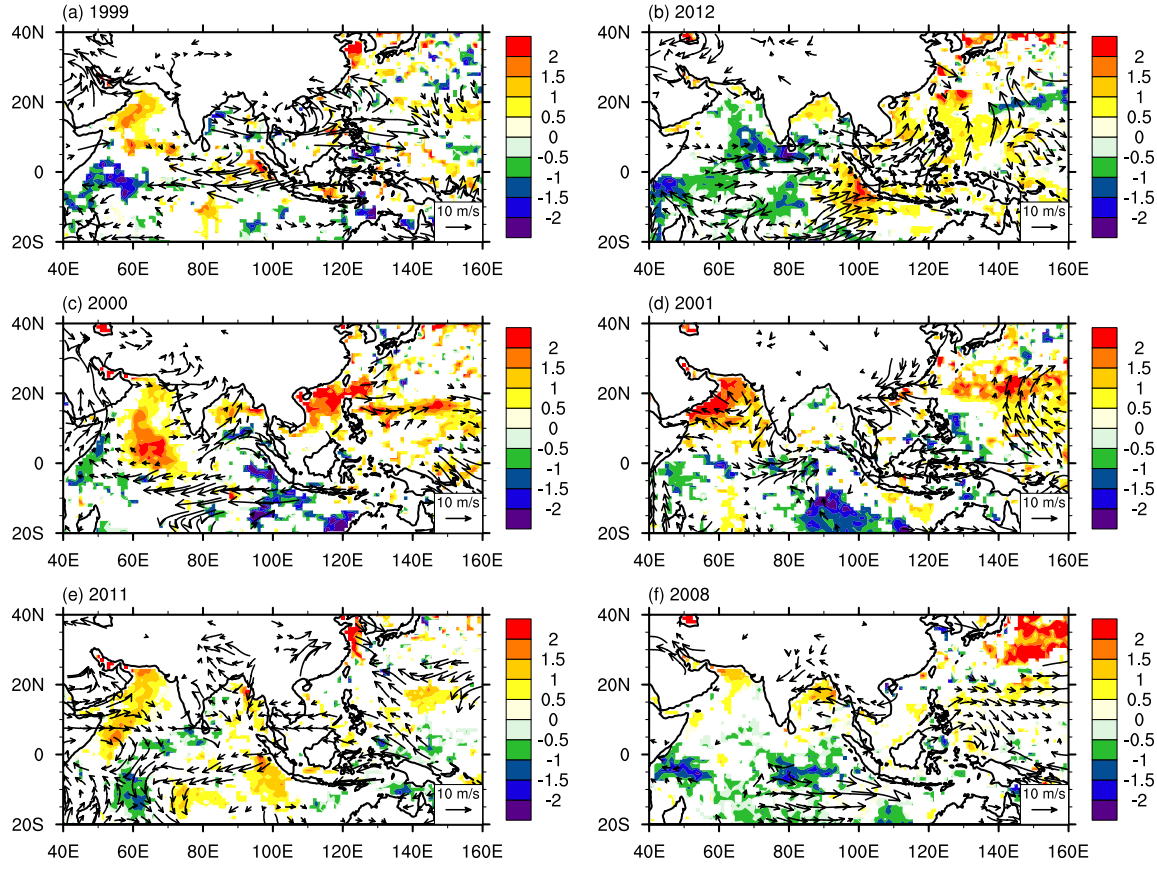

Figure 4. Linear trends in SST (shading; units: °C/10 d) and 850 hPa wind (vectors; units: m s^{-1}/10 d) for 15–24 April in years with a La Niña background state: (a) 1999; (b) 2012; (c) 2000; (d) 2001; (e) 2011; (f) 2008. Only values passing the 0.05 significance test are plotted.

locally in the normal onset type. In summary, the enhanced north–south thermal contrast over the Indian Ocean and the persistent warming over the SCS before the monsoon onset are the two key factors that control the behavior of the normal SCSSM onset type.

Previous studies (Xie et al. 1998; Zhou and Chan 2007) have also suggested that SCSSM onset tends to occur later (earlier) in years associated with an El Niño (La Niña) event, because the El Niño (La Niña) forces an equatorial westerly (easterly) anomaly that drives a weak (strong) Walker circulation, produces negative (positive) SST anomalies over the SCS, and favors a late (early) SCSSM onset. Our data-set includes five El Niño years (1998, 2003, 2005, 2007, and 2010) and six La Niña years (1999, 2000, 2001, 2008, 2011 and 2012). The SCSSM onset is indeed late in most of the El Niño years; however, onset is early only in 1999 and 2012, and is normal in other La Niña years. To understand the possible reasons for this, we plot in Figure 4 the linear trend in SST and 850 hPa wind for 15–24 April in each of these six years. In 1999 (Figure 4(a)), a cyclonic anomaly appears over the Indochina Peninsula, SCS, and WNP, while SST does not show a substantial trend in the Indian Ocean. The cyclonic anomaly is consistent with the propagation of precipitation seen in Figure 1(c), which suggests that the early onset in 1999 is a result of ISO activity. In 2012 (Figure 4(b)), SST shows a cooling trend throughout the Indian Ocean and warming trends at the west coast of Sumatra and in the SCS and WNP. This west–east thermal contrast triggers a westerly wind, which favors early onset in 2012. By contrast, in the other four years (Figure 4(c)–(f)), SST is either cooling near Sumatra and in the South Indian Ocean or is constant in the SCS, which prevents the generation of the westerly wind over the SCS and the early onset of the monsoon.

4. Summary

The interannual variability in the onset of the SCSSM from 1997 to 2014 is analyzed in this study. The U_{850} averaged over (5–20°N, 110–120°E) is used as the principal index for identifying the onset date. The evolutions of precipitation and SST are examined to understand the thermodynamics of the different onset processes. We separate the evolution of U_{850} into a seasonal transition phase and a monsoon onset phase: the seasonal transition can be clearly discerned in each year as the point of cessation of continuous easterly wind, but the establishment of a westerly wind and the development of monsoon precipitation vary greatly from year to year. Using four additional indices, we divide SCSSM onsets into three types. The mean state in normal onset cases is similar to that of intermittent onset cases, and is characterized by a well-established westerly wind over the entire Asian monsoon region. However, the precipitation pattern differs between the two types: precipitation displays a maximum over the SCS in the normal onset type, but vanishes in the same region in the intermittent onset type. The third type, delayed onset, occurs in 2014 only: the SCSSM begins 20 days after the TRD, due to an extension of the WPH. Additionally, ISO activity (in 1999) and the change in west–east thermal contrast across the Indian Ocean and western Pacific are found to affect the onset process in years with a La Niña background state.

This study describes the major thermodynamical features of the onset of the SCSSM. Monsoon onset is found to be sensitive to ENSO, local thermal contrasts, ISO activity, and the WPSH. Therefore, further studies are recommended on the relationships between monsoon indices and precursor signals in the atmosphere and ocean, with the aim of improving monsoon prediction.

Acknowledgements

We would like to thank the two anonymous reviewers for their constructive suggestions, which helped to improve the overall quality of the manuscript.

Disclosure statement

No potential conflict of interest was reported by the authors.

Funding

This study was jointly funded by the National Basic Research Program of China [grant number 2014CB953904], Strategic Priority Research Program of the Chinese Academy of Sciences [grant number XDA11010402], National Natural Science Foundation of China [grant numbers 41305068, 41405091, 41305065, and 91337110], and China Postdoctoral Science Foundation [2013M541011].

References

He, Z., and R. Wu. 2013. "Seasonality of Interannual Atmosphere–Ocean Interaction in the South China Sea." *Journal of Oceanography* 69: 699–712.

Hsu, H. H., C. T. Terng, and C. T. Chen. 1999. "Evolution of Large-scale Circulation and Heating during the First Transition of Asian Summer Monsoon." *Journal of Climate* 12: 793–810.

Hu, W. T., R. G. Wu, and Y. Liu. 2014. "Relation of the South China Sea Precipitation Variability to Tropical Indo-pacific SST Anomalies during Spring-to-summer Transition." *Journal of Climate* 27: 5451–5467.

Huffman, G. J., R. F. Adler, M. M. Morrissey, D. T. Bolvin, S. Curtis, R. Joyce, B. McGavock, and J. Susskind. 2001. "Global Precipitation at One-degree Daily Resolution from Multisatellite Observations." *Journal of Hydrometeorology* 2: 36–50.

Kajikawa, Y., and B. Wang. 2011. "Interdecadal Change of the South China Sea Summer Monsoon Onset." *Journal of Climate* 25: 3207–3218.

Kobayashi, S., Y. Ota, Y. Harada, A. Ebita, M. Moriya, H. Onoda, K. Onogi, et al. 2015. "The JRA-55 Reanalysis: General Specifications and Basic Characteristics." *Journal of the Meteorological Society of Japan. Ser. II* 93: 5–48. doi: 10.2151/jmsj.2015-001.

Lau, N. C., and M. J. Nath. 2000. "Impact of ENSO on the Variability of the Asian–Australian Monsoons as Simulated in GCM Experiments." *Journal of Climate* 13: 4287–4309.

Lin, P.-H., and H. Lin. 1997. "The Asian Summer Monsoon and Mei-Yu Front. Part I: Cloud Patterns as a Monsoon Index." *Atmospheric Sciences* 25 (2): 267–287.

Liu, B. Q., Y. M. Liu, G. X. Wu, J. H. Yan, J. H. He, and S. L. Ren. 2015. "Asian Summer Monsoon Onset Barrier and Its Formation Mechanism." *Climate Dynamics* 45: 711–726.

Mao, J. Y., and J. C. L. Chan. 2005. "Intraseasonal Variability of the South China Sea Summer Monsoon." *Journal of Climate* 18: 2388–2402.

Mao, J. Y., J. C. L. Chan, and G. X. Wu. 2004. "Relationship between the Onset of the South China Sea Summer Monsoon and the Structure of the Asian Subtropical Anticyclone." *Journal of the Meteorological Society of Japan* 82 (3): 845–859.

Reynolds, R. W., T. M. Smith, C. Y. Liu, D. B. Chelton, K. S. Casey, and M. G. Schlax. 2007. "Daily High-Resolution-blended Analyses for Sea Surface Temperature." *Journal of Climate* 20: 5473–5496.

Wang, B., and H. Lin. 2002. "Rainy Season of the Asian–Pacific Summer Monsoon*." *Journal of Climate* 15: 386–398.

Wang, B., H. Lin, Y. S. Zhang, and M. M. Lu. 2004. "Definition of South China Sea Monsoon Onset and Commencement of the East Asia Summer Monsoon*." *Journal of Climate* 17: 699–710.

Wang, B., R. G. Wu, and T. Li. 2003. "Atmosphere–Warm Ocean Interaction and Its Impacts on Asian–Australian Monsoon Variation*." *Journal of Climate* 16: 1195–1211.

Wen, M., T. Li, R. H. Zhang, and Y. J. Qi. 2010. "Structure and Origin of the Quasi-biweekly Oscillation over the Tropical Indian Ocean in Boreal Spring." *Journal of the Atmospheric Sciences* 67: 1965–1982.

Wu, R. G. 2010. "Subseasonal Variability during the South China Sea Summer Monsoon Onset." *Climate Dynamics* 34: 629–642.

Wu, R. G., and B. Wang. 2001. "Multi-stage Onset of the Summer Monsoon over the Western North Pacific." *Climate Dynamics* 17: 277–289.

Wu, G. X., and Y. S. Zhang. 1998. "Tibetan Plateau Forcing and the Timing of the Monsoon Onset over South Asia and the South China Sea." *Monthly Weather Review* 126: 913–927.

Xie, A., Y.-S. Chung, X. Liu, and Q. Ye. 1998. "The Interannual Variations of the Summer Monsoon Onset Overthe South China Sea." *Theoretical and Applied Climatology* 59: 201–213.

Zhou, W., and J. C. L. Chan. 2007. "ENSO and the South China Sea Summer Monsoon Onset." *International Journal of Climatology* 27: 157–167.